Dalton Transactions

Accepted Manuscript

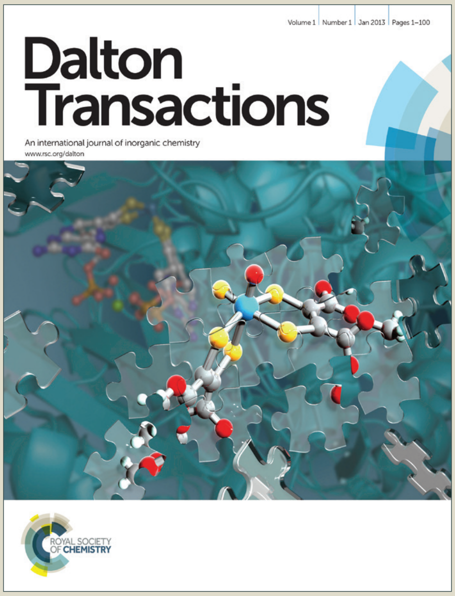

ROYAL SOCIETY OF CHEMISTRY

www.rsc.org/dalton

Bismuth Induced Enhanced Green Emission from Terbium ion and its Complex in Thin Film

Gagandeep Kaur, Brijesh Kumar, R. K. Verma and S. B. Rai*
Laser and Spectroscopy Laboratory, Physics Department,
Banaras Hindu University, Varanasi 221005, India

Abstract

Bismuth nanoparticles (NPs) have been prepared by pulsed laser ablation technique using third harmonics of Nd-YAG laser. UV-absorption and TEM micrographs show Bi NPs of spherical shape with average particle size ranging from 15-20 nm. These NPs were dispersed with Tb^{3+} ions and its complex with Salicylic acid (Sal) in Polyvinyl alcohol to obtain thin films. The influence of Bi NPs on the emissive properties of Tb^{3+} ions and $[Tb(Sal)_3(phen)]$ complex has been studied by luminescence spectroscopy using 266 nm and 355 nm as excitation wavelengths. The luminescence intensity of Tb^{3+} ion complexed with Sal in the thin polymer films is increased significantly as compared to the Tb^{3+} ion in the presence of Bi NPs on excitation with 355 nm. However, terbium ions in case of $[Tb(Sal)_3(phen)]$ complex together with NPs show an intense and extended emission spectrum in the 375–700 nm range for transitions arising from $^5D_3$ and $^5D_4$ levels to different ^7F_J levels on 266 nm excitation. The luminescence enhancement has also been supported by life time measurements.

Keywords: Nanoparticles; Laser processing; Polymers; Luminescence; Thin films.

*Corresponding author**:** - Tel.: +91 – 542 - 2307308; Fax: +91 – 542 – 2368390

Email: sbrai49@yahoo.co.in

1. Introduction

Optically-active polymer materials doped with lanthanide (Ln^{3+}) ions are suitable for use in varied optoelectronic applications such as amplifiers, fibers, waveguides etc., due to their low cost and ease of processing [1, 2]. Ln^{3+} ions give intense narrow spectral emissions from long lived excited-state arising from partially filled $4f^n$ orbitals [3]. These advantageous radiative properties of Ln^{3+} ions unfortunately tend to be suppressed by the inherently high vibrational frequencies of different bonds of polymers when added to the polymer host. Additionally, Ln^{3+} ion salts exhibit limited solubility in polymers and tends to aggregate resulting in enhanced scattering and luminescence quenching even at low concentrations. Thus to avoid this, Ln^{3+} ions before being dispersed in polymeric hosts are combined with an organic ligand which absorbs the incident light energy and transfers it to the Ln^{3+} ion. One such ligand is Salicylic acid (hereafter Sal), a carboxylic acid with the aromatic ring, which increases the energy absorbed by the Ln^{3+} ion and hence, the observed luminescence. There are absorption in the UV spectral region on the aromatic ring and then transfer energy to the trivalent lanthanide ions. Thus Ln^{3+} coordinated complexes in polymer hosts are used for numerous practical applications and their luminescence efficiency may be improved by a variety of methods [2- 5]. Any effort to improve the efficiency by increasing the Ln^{3+} concentration, does not succeed as aggregation of ions takes place at higher concentration and act as quenching centers.

Luminescent nanoscale materials in the form of nanoparticles (NPs) are of interest not only for basic research but also enables several applications such as optical amplifiers, colored displays, lasers etc., affecting the luminescence and dynamics of the optically active materials. These phenomena are related to the energy transfer between the NPs and lanthanide ions and/or the enhancement of local energy field that acts on the ions located in their proximity specifically when the wavelength of the incident light beam or luminescent wavelength is close to their surface plasmon resonance wavelength [6, 7]. High surface-to-volume ratio, local phenomenon such as absorption or change in the surface electronic state may contribute significantly to special properties. Metallic and semi-metallic NPs are attractive because their physical properties are very different from those of the bulk due to quantum size effect. Bismuth is a semimetal with a small energy overlap between the conduction and valence bands, size induced semimetal to semiconductor transition and the related quantum confinement effects are potentially useful for optical and electro-optical device applications [8-12].

The luminescent complexes of inorganic species with ligands in different media and adding NPs to it open up the possibilities of increasing the luminescence by several orders of magnitude. Many studies have been carried out on the enhancement of optical properties of Ln^{3+} ions and their complexes in different matrices [13-15]. In the present study, spherical Bi NPs in water were prepared by laser ablation and then dispersed with Tb ions and $[Tb(Sal)_3(phen)]$ complex in the polymer host, Polyvinyl Alcohol (PVA) to obtain thin films. The luminescence spectra of the prepared films have been monitored using 266 nm (resonant with SPR band of Bi NPs) and 355 nm (off-resonant) radiations for excitation. Here we report the luminescence enhancement of terbium ions and its complex in the presence of bismuth NPs embedded in polymer host.

2. Materials and Method

Terbium oxide and Salicylic acid used are 99.9 % pure while 1, 10-phenanthroline is 99.5 % pure (all purchased from Sigma Aldrich) and used without further purification. Bismuth plate (99.0 %) obtained from the same firm was used for laser ablation.

Preparation of Bi nanoparticles: Spherical Bi NPs were prepared using laser ablation from a bismuth plate (diameter ~ 20mm and thickness ~ 2.0mm) immersed in water (3 mm below the air-water interface) kept in a glass beaker. The bismuth target was irradiated by 355 nm radiation from a pulsed Nd:YAG laser (repetition rate 10 Hz, pulse width 7 ns and pulse energy ~ 80 mJ). The laser beam was focused on the metal target to within 1-4 mm diameter spot with a 15 cm focal length lens while the target plate was kept rotating during the ablation. As the laser pulse strikes the silver target, a characteristic cracking sound emanated. The pulsed laser ablation technique is shown in Fig. 1(A). A comparison of fresh water and Bi NPs in water showing change in color of the solution to light brown is made in Fig. 1(B).

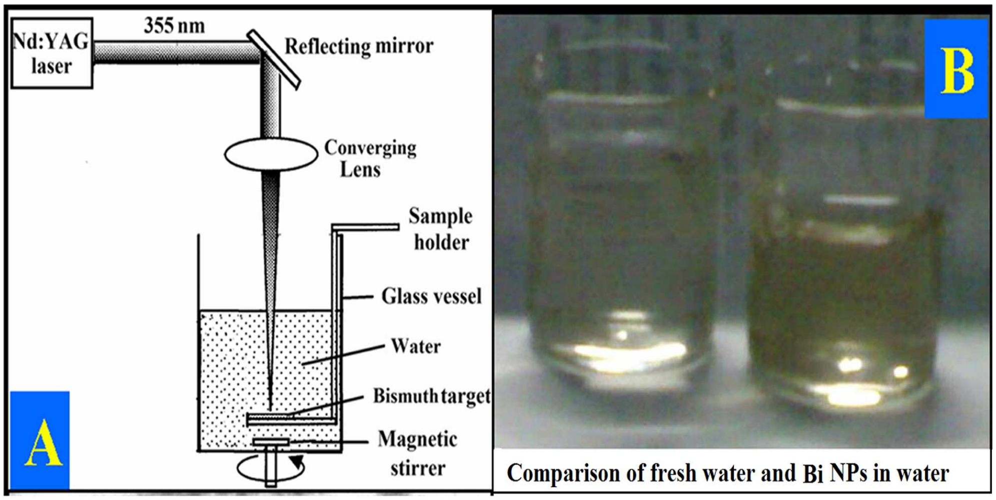

Comparison of fresh water and Bi NPs in water

Fig. 1 (A) Experimental setup for laser ablation of bismuth target in water for preparation of NPs. (B) A comparison of pure water and water containing Bi NPs showing change in color of the solution to light brown.

Preparation of [Tb(Sal)$_3$(phen)] complex: 0.013 mmol of Tb_4O_7 was obtained by dissolving Tb_4O_7 in concentrated hydrochloric acid (HCl). 0.018 mmol of Salicylic acid and 0.006 mmol of 1, 10-phenanthroline were separately dissolved in 2.0 ml ethanol. This ethanolic solution was added drop wise to $TbCl_3$ and stirred for half an hour to get Tb(Sal)$_3$Phen complex (as described in reference 16).

Preparation of PVA sample with Tb complex and Bi nanoparticles: 0.011 mmol of PVA was dissolved in distilled water to obtain transparent homogeneous solution. Separately, the ethanolic solution of as-prepared [Tb(Sal)$_3$(phen)] complex was mixed with 0.5 mol % of laser ablated Bi nanoparticles in water. This mixture was homogenized at room temperature using a magnetic stirrer for two hours and was poured into aqueous solution of PVA. The resulting solution was stirred rigorously for 4-5 hrs and then poured into a Petri dish and allowed to dry overnight to get thin films.

Characterization: Absorption spectra were recorded using Cary 2390 double beam UV-Vis-NIR spectrophotometer. Transmission electron micrographs were taken using Technai 20G2 (Philips) transmission electron microscope (TEM) equipped with the charge coupled device (CCD). For excitation spectra and lifetime measurements, a Fluorolog–3 Spectrofluorometer (FL3-11, Horiba JobinYvon Edison MJ USA] was used. Third and fourth harmonics from Nd:YAG laser [Spitlight-600, Innolas, Germany] with

Spectrofluorometer [Flouromax–4, Horiba Jobin Yvon] was used for recording the luminescence.

3. Results and discussions

3.1. Structural analysis using Transmission Electron Microscopy (TEM):

Transmission Electron Microscopy was performed for the evaluation of shape and size of Bi NPs. The TEM micrographs in Fig. 2 show spherical Bi NPs with average particle size in the range between 15 ± 3.4 nm and 20 ± 2.8 nm. Some particles also seem to be agglomerated leading to bigger particle size in the micrograph.

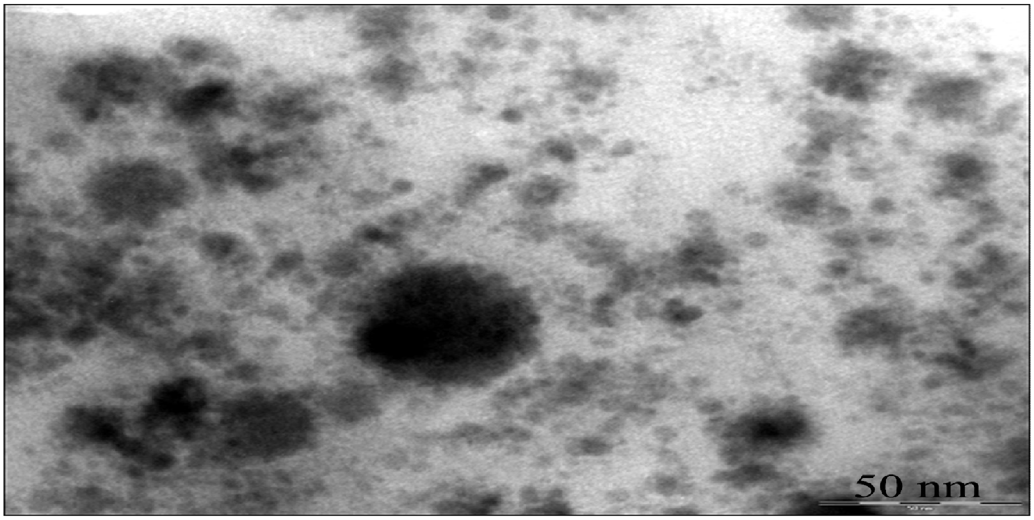

Fig. 2: Transmission Electron Microscopy (TEM) image of Bi NPs in water prepared by 355 nm laser ablation.

3.2. Optical characterization:

3.2.1. UV-Vis absorption:

The surface plasmon resonance is a characteristic of NPs embedded in a dielectric host and is attributed to the collective oscillation of electrons in response to optical excitation. Fig. 3 shows the absorption spectra of Bi NPs in water ablated for 20 min., of the [Tb(Sal)$_3$(phen)] complex in PVA and of [Tb(Sal)$_3$(phen)] complex with Bi NPs in PVA. The absorption spectrum of Bi NPs in water show typical surface plasmon resonance absorption at 267 nm alongwith a small band at 283 nm which may be assigned to $^4S_{3/2} \rightarrow ^2P_{3/2}$ of Bi^0 transitions [17]. After ablation of the bismuth target for 40 min., the peak at 267 nm is observed to diminish and the intensity of peak at 283 nm started increasing which indicates that the Bi^{3+} ions are reduced completely to bismuth NPs [18-21]. Also, it is observed that the NPs get agglomerated giving bigger size of NPs on ablation for a longer period and hence, absorption at a longer wavelength. M.Gutiérrez *et al.* [22] reported that nanometer-sized bismuth particles exhibited an absorption at ~253 nm and according to J. A. Creighton *et al.* [23], the first absorption band of 10 nm bismuth particles should appear around 270 – 280 nm. Wang *et al.* [18] have synthesized poly (vinylpyrroldone) stabilized bismuth NPs with absorption peak at 281 nm. Our result fits well with the above two literature values.

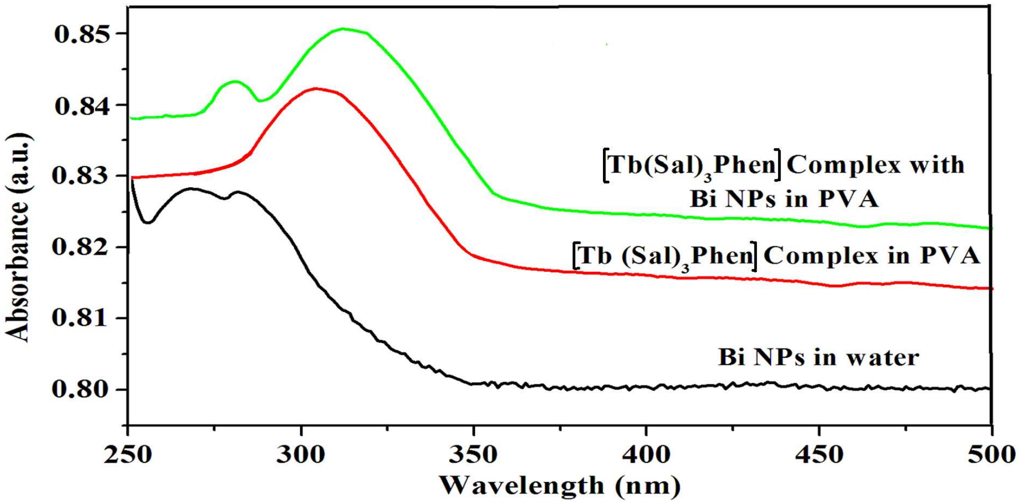

Fig. 3: Absorption spectra of Bi NPs in water ablated for 20 min. of the [Tb(Sal)$_3$(phen)] complex in PVA and of [Tb(Sal)$_3$(phen)] complex with Bi NPs in PVA.

The [Tb(Sal)$_3$(phen)] complex in PVA film shows a band centered at 315 nm due to the $S_0 \rightarrow S_1$ absorption of Salicylic acid (Sal) overlapping the absorption band due to $\pi \rightarrow \pi^*$ transition of PVA. The absorption spectrum of [Tb(Sal)$_3$(phen)] complex with Bi NPs in PVA show the absorption peak for Bi NPs with the absorption peak due to Sal which shows a red shift of ~8 nm when Bi NPs are also embedded in the PVA film alongwith [Tb(Sal)$_3$(phen)] complex. This shift is attributed to an aggregation of the complex through NPs [24].

The average radius of Bi NPs can be estimated using the absorption of plasmon band as

$$r = AV_F \;/2\pi c(\Delta\lambda/\lambda_P^2) \qquad (1)$$

Where A is the line broadening constant, V_F is the Fermi velocity of electrons and its value is 1.87×10^6 m/s for bismuth nanoparticles, c is the velocity of light, λ_P is the plasmon resonance wavelength, and $\Delta\lambda$ is the full width at half maxima of Bi NPs plasmon resonance peak. The calculated average radius of Bi nanoparticles is ~18.5 nm.

3.2.2. Excitation spectra

The excitation spectra of Tb ion in PVA, Tb ion with Bi NPs in PVA and [Tb(Sal)$_3$(phen)] complex with Bi NPs in PVA corresponding to $^5D_4 \rightarrow {}^7F_5$ (544 nm) transition of Tb^{3+} ion were recorded and are shown in **Fig. 4**.

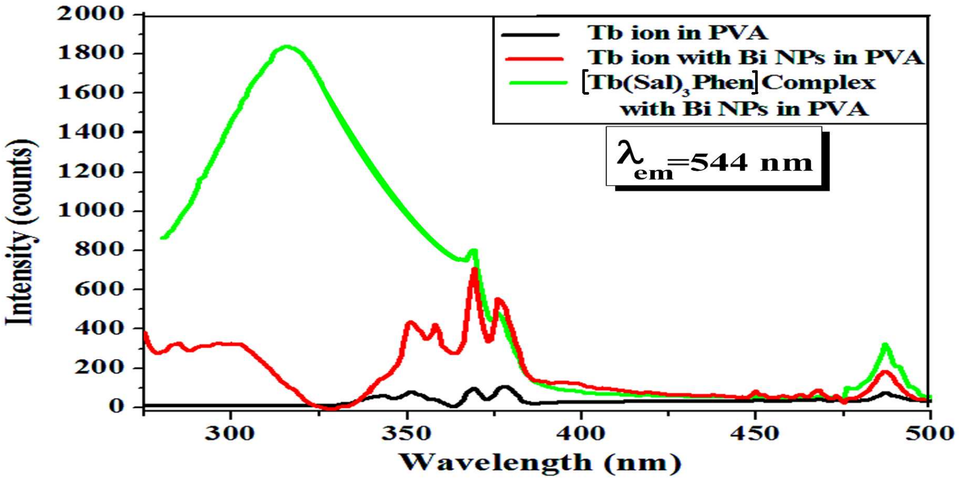

Fig. 4: Excitation spectra of Tb ion in PVA, Tb ion with Bi NPs in PVA and [Tb(Sal)$_3$(phen)] complex with Bi NPs in PVA corresponding to $^5D_4 \rightarrow ^7F_5$ (544 nm) transition of Tb^{3+} ion.

The excitation spectrum of Tb ion in PVA sample shows few weak bands at 341, 352, 358, 369, 377 and 488 nm wavelengths corresponding to absorption of Tb^{3+} ion. It is interesting to note that on addition of Bi NPs to TbCl$_3$, the excitation intensity of the bands was observed to improve alongwith a weak band for Bi NPs at 285 nm. The excitation spectrum of [Tb(Sal)$_3$(phen)] complex with Bi NPs in PVA shows an excitation broad band ranging from 275-375 nm due to n→π* transition of salicylate ligand. The intensity enhancement of the bands corresponding to the Tb^{3+} ion emission clearly indicate effective sensitization of Tb^{3+} ions by the ligands, pointing to an efficient antenna effect [25].

3.2.3. Photoluminescence on 266 nm excitation

Fig. 5 shows the emission in the luminescence spectra of Tb^{3+} ion, Tb^{3+} ion with Bi NPs and [Tb(Sal)$_3$(phen)] complex with Bi NPs in PVA in the range of 375–700 nm on excitation of the SPR band of NPs using 266 nm radiation. The spectra of Tb^{3+} ion exhibit characteristic emission peaks at 487, 544, 583 and 618 nm of Tb^{3+} ions emanating from $^5D_4 \rightarrow ^7F_J$ (J=6, 5, 4, 3) transitions respectively and among them $^5D_4 \rightarrow ^7F_5$ transition (544 nm) is the most intense one. Adding Bi NPs enhances the emission intensity of Tb^{3+} bands but the effect is more pronounced in case of $[Tb(Sal)_3(phen)]$ complex in PVA with an additional interesting feature showing emission from $^5D_3$ level also.

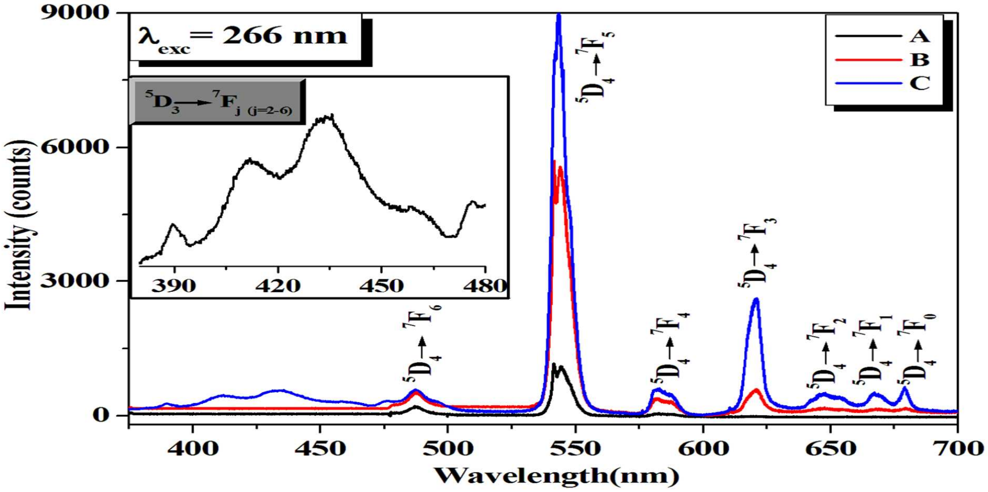

Fig. 5: Luminescence spectra of Tb ions (A), Tb ions with Bi nanoparticles (B) and $[Tb(Sal)_3(phen)]$ complex with Bi NPs (C) in PVA in the range of 375-700 nm on excitation of the SPR band of NPs using 266 nm.

The mechanism of enhancement of the emission intensity of observed transitions can be explained with the help of partial energy level diagram in Fig. 6 showing different routes of excitation of Tb^{3+} ion. Initially 266 nm photon excites the $^5H_7$ level through $^7F_6 \rightarrow ^5H_7$ absorption transition of Tb^{3+} ions where from the excited Tb^{3+} ions relax non-radiatively down to $^5D_3$ and $^5D_4$ levels to get the emissions to lower lying levels (^7F_J ; J =1-

6). The 266 nm radiation also excites the surface plasmon band of Bi NPs. The excitation energy is transferred from the SPR band of Bi NPs to Tb^{3+} ions which enhance the population of upper level of Tb ion in $^5D_3$ and $^5D_4$ levels and increase the luminescence intensity. The large absorption cross section of the bismuth plasmon band causes an increased excitation of $^5D_4$ level of Tb ion via energy transfer from the excited SPR level of Bi NPs. The ligand Sal does not absorb at 266 nm excitation as no energy level of Sal exists at this energy. It simply encapsulates the Tb ion from the host vibrations and intensifies the emission in the complexed Tb ion and emergence of emission from $^5D_3$ level.

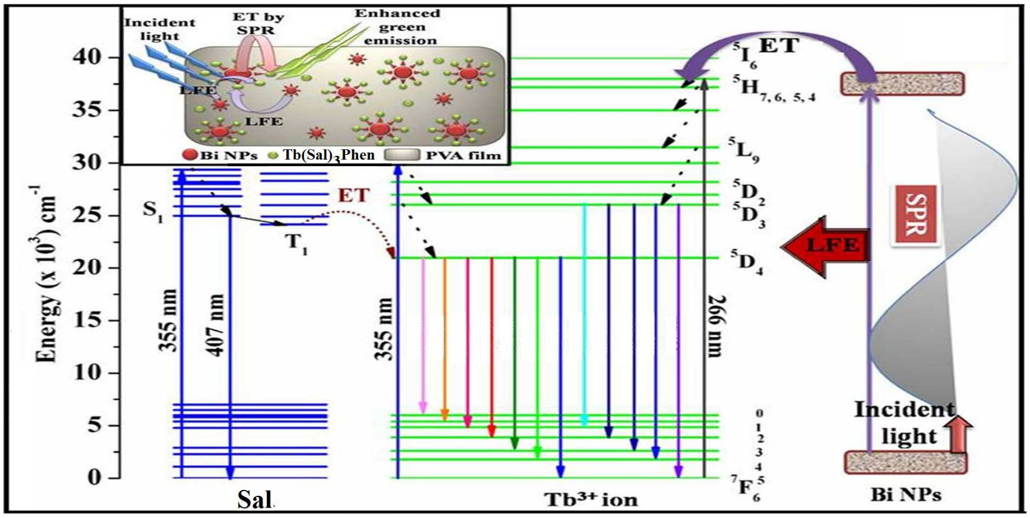

Fig. 6: Partial energy level diagram showing different routes of excitation of Tb ion for the enhanced green emission on excitation with 266 / 355 nm exciting SPR of Bi NPs and Sal ligand respectively. Inset of Fig. shows the Tb ions, Bi NPs, and $[Tb(Sal)_3(phen)]$ complex in PVA host showing plasmonic field effect to enhance the emission of Tb ion energy transfer (ET) where SPR refers to Surface Plasmon Resonance, LFE stands for Local Field Effect.

3.2.4. Photoluminescence on 355 nm excitation

Fig. 7 shows the luminescence spectra for emission of Tb ion, Tb ion with Bi NPs, [Tb(Sal)$_3$(phen)] complex with Bi NPs in PVA in the range of 375–700 nm on excitation with 355 nm radiation. Though the emission spectra resemble the earlier one but the emission intensity is much more enhanced for [Tb(Sal)$_3$(phen)] complex with Bi NPs. The observed enhancement in the emission intensity may be understood as follows: The 355 nm radiation excites both the Tb^{3+} ion as well as ligand Sal to the excited state while Bi NPs do not absorb this wavelength. The incident energy absorbed directly by $^5L_9$ level of Tb^{3+} ions populates the emitting $^5D_4$ level and the optical energy absorbed by the Sal ligand is also transferred to Tb^{3+} ions populating the $^5D_4$ level via intersystem crossing and subsequent energy transfer process thus enhancing the emission intensity [3]. The Bi NPs form a local plasmonic field around the [Tb(Sal)$_3$(phen)] complex and the high field gradients of NPs increase the lifetime of the emitting level of Tb^{3+} ion [5, 26]. The strong coupling between the radiative transitions and the field effect is the basic cause of the intensity enhancement as shown in the inset to Fig. 6. The increase in the lifetime of $^5D_4$ level of Tb^{3+} is clearly seen in the decay curve of $^5D_4 \rightarrow {}^7F_5$ transition with and without Bi NPs (see Fig. 8).

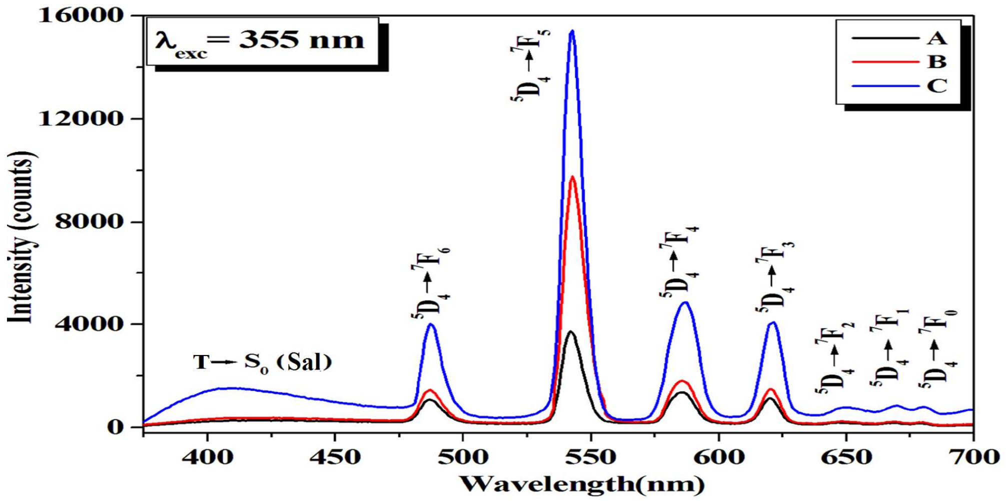

Fig. 7: Luminescence spectra of Tb ion (A), Tb ion with Bi NPs (B), [Tb(Sal)$_3$(phen)] complex with Bi NPs (C) in PVA in the range of 375-700 nm on excitation with 355 nm radiation.

It is interesting to note that the different transitions of Tb^{3+} ion are affected differently by the NPs. This is because the magnetic dipole allowed transition differs in interaction with surface plasmon field as compared to the electric dipole allowed transitions. However the intensity of Tb^{3+} bands using 355 nm excitation is much larger than using 266 nm excitation. This clearly demonstrates that the energy transfer through the ligand Sal is much efficient than through other channels.

3.2.5. Time resolved photoluminescence spectroscopy

Fig. 8 depicts the decay curves for $^5D_4 \rightarrow {^7F_5}$ transition at 544 nm of Tb^{3+} ions with and without Bi NPs and [Tb(Sal)$_3$(phen)] complex with Bi NPs in PVA using pulsed 355 nm radiation. A first order exponential decay fit for the curves leads to a larger life time (of $^5D_4$

level) in the presence of NPs. The values obtained for lifetimes with respective values of standard deviation are as follows:

Tb^{3+} ions in PVA : Lifetime: 287 μs, Standard deviation: 3.67 μs

Tb^{3+} ions with Bi NPs in PVA: Lifetime: 399 μs, Standard deviation: 9.25 μs

[Tb(Sal)$_3$(phen)] in PVA : Lifetime: 625 μs, Standard deviation: 5.45 μs

[Tb(Sal)$_3$(phen)] with Bi NPs in PVA: Lifetime 659 μs, Standard deviation 6.76 μs

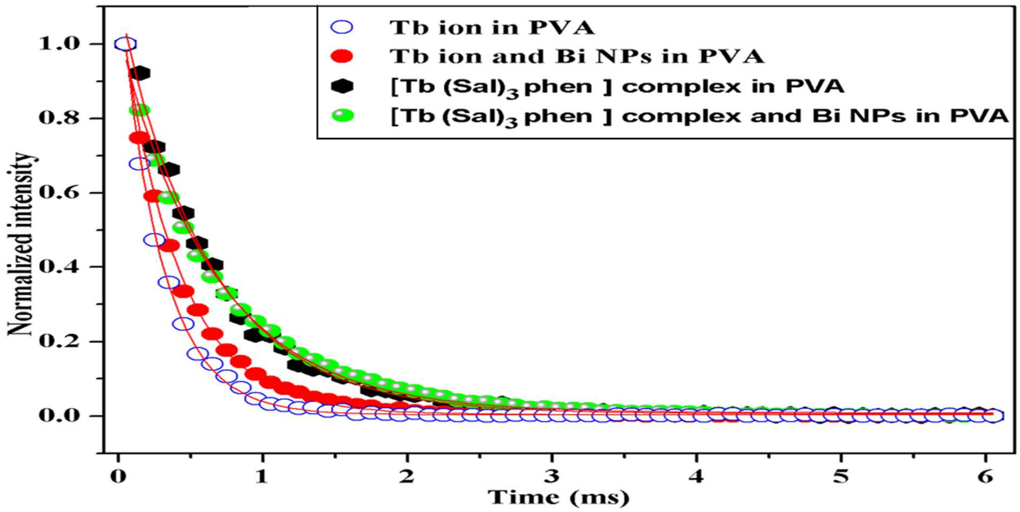

Fig. 8: The decay curve for $^5D_4 \rightarrow {}^7F_5$ transition at 544 nm of Tb^{3+} ions with and without NPs and [Tb(Sal)$_3$(phen)] complex with and without Bi NPs in PVA using 355 nm radiation.

The increment in lifetime is explained as due to the local surface fields of Bi NPs as given in the inset of Fig. 6 demonstrating that the luminescence properties of polymer doped Ln^{3+} complexes can be improved by adding NPs [5]. There is good improvement in the lifetime values when Bi NPs are added to the $TbCl_3$ in PVA and on the other hand for the [Tb(Sal)$_3$(phen)] complex there is just a small increase in the lifetime.

4. Conclusions

To summarize, Tb ion and its organic complex with salicylic acid has been dispersed separately with Bi NPs in PVA polymer film at room temperature. Optical absorption and TEM micrographs confirm the formation of spherical Bi NPs with size lying in the range 15-20 nm. The emission efficiency of Tb^{3+} ion and its complex is seen to be enhanced in the presence of Bi NPs on pumping with 266 and 355 nm radiations. $[Tb(Sal)_3(phen)]$ complex with Bi NPs show an extended emission spectrum of Tb^{3+} ion in the 375–700 nm range from $^5D_3$ and $^5D_4$ levels to different ^7F_J levels on 266 nm excitation. But the enhancement is larger for $[Tb(Sal)_3(phen)]$ complex using 355 nm excitation. This is attributed to the coupling of plasmonic field effects of Bi NPs on Tb^{3+} ions which affect the lifetime of the radiative level as well as energy transfer from Sal to Tb^{3+}.

Acknowledgements

B. Kumar would like to acknowledge UGC for RFSMS fellowship. G. Kaur is grateful to DST, India, for financial assistance in the form of project grant as WOS-A.

References

[1] K. Binnemans. Chem. Rev. 109 (2009) 4283-4374.

[2] K. Gipson, C. Kucera, D. Stadther, K. Stevens, J. Ballato, P. Brown. Polymers 3 (2011) 2039-2052.

[3] G. Kaur, S. B. Rai. J. Phy. D: Appl. Phys. 44 (2011) 425306-6.

[4] V. Bekiari, P. Lianos. J. Lumin. 101 (2003)135-140.

[5] G. Kaur, R. K. Verma, D. K. Rai, S. B. Rai. J. Lumin. 132 (2012) 1683-1687.

[6] D. M. Silva, L. R. P. Kassab, S. R. Lüthi, C. B. Araújo, A. S. L. Gomes, M. J. V. Bell. Appl. Phys. Lett. 90 (2007) 081913-3.

[7] B. Kumar, G. Kaur, S. B. Rai, Appl. Phys. B 110 (2013) 345-351.

[8] L. Balan, R. Schneider, D. Billaud, Y. Fort, J. Ghanbaja. Nanotechnology 15 (2004) 940-944.

[9] J. Fang, K. L Stokes, J. A. Wiemann, W. L. Zhou, J.Dai, F. Chen, C. J. O'Connor, Mater. Sci. Eng. 2001, B83, 254.

[10] R. Serna, J. C. G. De Sande, J. M. Ballesteros, C. N. Afonso, J. Appl. Phys. 1998, 84, 4509.

[11] S.Sivaramakrishnan, V. S.Muthukumar,; S.Sivasankara, K.Venkataramaniah, J. Reppert, A. M.Rao, M.Anija, R.Philip, N.Kuthirummal, Appl. Phys. Lett. 2007, 91, 093104.

[12] E. Haro-Poniatowski, R. Serna, M. J. de Castro, A. Suárez-García, C. N. Afonso, I. Vickridge, Nanotechnology, 2008, 19, 485708.

[13] R. Reisfeld, T. Saraidarov. Opt. Mat. 28 (2006) 64-70.

[14] R. Reisfeld, M. Pietraszkiewicz, T. Saraidarov, V. Levchenko. J. Rare Earths 27 (2009) 544-549.

[15] A. J. Silversmith, D. M. Boye, K. S. Brewer, C. E. Gillespie, Y. Lu, D. L. Campbell. J. Lumin. 121 (2006) 14-20.

[16] G. Kaur, Y. Dwivedi, S. B. Rai, Optics Comm. 283 (2010) 3441.

[17] M. Peng, C. Zollfrank, L. Wondraczek, J. Phys.: Condens. Matter. 21 (2009) 285106, 1-6.

[18] Y. W. Wang, B. H. Hong, K. S. Kim. J. Phys. Chem. B. 109 (2005) 7067-7072.

[19] J. C. G. De Sande, T. Missana, C. N. Afonso, J. Appl. Phys.1996, 80, 7023.

[20] O. Hunderi, J. Phys. F 1975, 5, 2214.

[21] J. Toudert, R. Serna, M. J. de Castro, J. Phys. Chem. C 2012, 116, 20530−20539.

[22] M.Gutiérrez, A. Henglein, J. Phys. Chem., 100(1996) pp. 7656 – 7661.

[23] J. A. Creighton, G. E. Desmond, J. Chem. Soc. Faraday Trans., 87(24)(1991) 3881 – 3891.

[24] J. Chang, J. Dong, Spectrum, Principle and Analysis, Scientific Press, China, 2001.

[25] G. Kaur, Y. Dwivedi, S. B. Rai, Mat. Chem. Phys. 130 (2011) 1352

[26] Q. Wang, F. Song, S. Lin, C. Ming, H. Zhao, J. Liu, C. Zhang, E. Y. B. Pun. J. Nanopart. Res. 13 (2011) 3861-3865.